American Mineralogist, Volume 64, pages 573–586, 1979

Thermal expansion and high-temperature crystal chemistry of the Al_2SiO_5 polymorphs

JOHN K. WINTER AND SUBRATA GHOSE

Department of Geological Sciences, University of Washington
Seattle, Washington 98195

Abstract

The crystal structures of sillimanite and andalusite have been refined from intensity data collected at 25, 400, 600, 800, and 1000°C. *R* factors following refinement were 0.033±.002 and 0.029±.002 for the sillimanite and andalusite data sets respectively. For kyanite 2140, 1773, and 1741 reflections were measured at 25, 400, and 600°C, and the final *R* factors were 0.033, 0.031, and 0.036 respectively.

Unit-cell dimensions of all three polymorphs vary linearly with temperature. Although the unit-cell dimensions determined at room temperature agree within error limits with those of Skinner *et al.* (1961), significant deviations occur between the two data sets at elevated temperatures. All the Al octahedra exhibit considerable expansions with increasing temperature. In contrast, Al- or Si-tetrahedra in all three polymorphs remain relatively constant in size and shape as temperature is increased. Within the five-coordinated Al_2 polyhedron in andalusite the four short bonds remain relatively unchanged, whereas the longest bond, Al_2–O_C, expands considerably. The orientation of the long Al_1–O_D bonds in sillimanite and andalusite, which are more expandable than the other octahedral Al–O bonds, determines the direction of maximum unit-cell expansion. The chains of fully stretched tetrahedra (and Al_2 trigonal bipyramids in andalusite) restrict expansion in the *c* cell direction for these two minerals. The greater number of shared octahedral edges in kyanite, as well as the lack of continuous tetrahedral chains, results in more evenly distributed coefficients of unit-cell expansion.

Polymorphic transitions involve major reconstructive transformations. In addition, the andalusite–sillimanite transition requires diffusive interchange of half the Si and Al_2 atoms. Consequently, although metastable coexistence of two or three polymorphs is commonly observed, coherent replacement textures are rare. The present volume–temperature data agree well with the experimentally-derived thermodynamic properties of the aluminum silicate minerals.

Introduction

Andalusite, kyanite, and sillimanite, the three Al_2SiO_5 polymorphs that commonly occur in metamorphosed pelitic sediments, have been the subject of a great deal of study in the fields of metamorphic and experimental petrology. Due to the small changes in thermodynamic properties associated with the polymorphic phase transitions, metastable coexistence of these phases is common, and the mode of occurrence and relative fields of stability of the polymorphs are not completely clear.

The crystal structures of sillimanite and andalusite were first determined by Taylor (1928, 1929), using estimated intensities from rotation photographs. The kyanite structure was deduced by inference from the staurolite structure by Naray-Szabo *et al.* (1929). From diffractometer-counter data, the structures of andalusite, sillimanite, and kyanite were refined by Burnham and Buerger (1961) and Burnham (1963a, b) respectively. Refinements of sillimanite and andalusite structures based on neutron diffraction data have been performed by Finger and Prince (1972). Thermal expansions of the three polymorphs were determined by Skinner *et al.* (1961), using the powder-diffraction technique with a heating stage.

We wish to relate the details of the crystal structures of the three polymorphs determined at elevated temperatures to the thermal expansion data, and thereby provide a basis for understanding the behav-

0003-004X/79/0506-0573$02.00

ior of these polymorphs at high temperatures. All three polymorphs have one Al atom in six-coordination and one Si atom in four-coordination. The major difference in their crystal structures is due to the coordination of the remaining Al atom, which is four in sillimanite, five in andalusite, and six in kyanite. The thermal expansions, distortions, and orientations of the various Si and Al coordination polyhedra can be related to the changes in unit-cell dimensions as temperature increases. These relationships are expected to provide a better understanding of the causes and mechanisms of the polymorphic transformations.

Experimental

Collection of intensity data

The andalusite used was a large, clear, light pink crystal from Minas Gerais, Brazil (S. Ghose collection). Several fragments were ground to spheres by the method of Bond (1951). A sphere of 250μm diameter was selected for analysis and the quality of crystallinity checked by transmission Laue photographs. The crystal sphere was cemented to a silica-glass fiber and sealed in an evacuated silica-glass capillary. Sillimanite from Brandywine Springs, Delaware (University of Chicago #2261) was light brown and contained small, rod-like lamellae of quartz (<5 percent by volume). A relatively quartz-free cube of suitable crystallinity and about 280μm in diameter was selected and mounted in a silica-glass capillary. Kyanite proved to be considerably more difficult to work with. Several samples were crushed and carefully searched for fragments suitable for single-crystal X-ray analysis. However, severely bent crystals were common, presumably the result of crushing. Finally, careful crushing of a sample from Burnsville, North Carolina (Smithsonian Institution, NMNH #121285) produced small fragments displaying fewer deformational effects. A nearly cubic fragment just under 200μm along an edge was found which produced sharp Laue diffraction spots. This crystal was mounted directly in an evacuated silica-glass capillary.

Details of the single-crystal microfurnace and the procedures used for X-ray intensity data collection at high temperatures are given by Winter *et al.* (1977). The refinement of unit-cell dimensions of all three polymorphs was based on 15 reflections evenly distributed in a quadrant of reciprocal space between 18 and 50° 2θ (Mo$K\alpha$). For the intensity data collection, a variable 2θ scan rate of 2°/minute minimum was used along with graphite-monochromatized Mo$K\alpha$ radiation. Intensity data of reflections between 2 and 65° 2θ were collected for andalusite and sillimanite. 2140 reflections were measured for the kyanite sample within this range at room temperature; higher-temperature data collections were limited to $2\theta = 60°$ to prolong furnace life. Intensity data for andalusite and sillimanite were collected at 25, 400, 600, 800, and 1000°C. Kyanite data were collected at 25, 400, and 600°C. During the 800°C run, the microfurnace failed, having served for several months at temperatures up to 1080°C.

Refinement of the crystal structures

Corrections for Lorentz and polarization effects (but not for absorption and extinction) were applied, and the intensity data were converted to structure factors. Full-matrix least-squares refinements using the initial atomic coordinates and anisotropic temperature factors of Burnham and Buerger (1961) and Burnham (1963a,b) for andalusite (space group *Pnnm*), sillimanite (space group *Pbnm*), and kyanite (space group $P\bar{1}$) respectively, were performed using the program RFINE (Finger, 1969). Atomic scattering factors for Al, Si, and O atoms were taken from Cromer and Mann (1968), and anomalous dispersion corrections were made according to Cromer and Liberman (1970). The observed structure factors (F_o's) were weighted by $1/\sigma^2(F_o)$, where $\sigma(F_o)$ is the standard deviation of F_o as measured by counting statistics. Three cycles of scale factor refinement followed by three cycles of anisotropic temperature factor refinement varying atomic positions only were made prior to full refinement. Convergence was attained using four or fewer cycles of full anisotropic temperature factor refinement. The glass wall of the microfurnace produces a halo of diffuse-scattered X-rays which may have interfered with the intensity measurements of a few reflections. Due to possible errors resulting from this effect or from secondary extinction, all reflections with $|F_o - F_c| > 5.0$ were rejected in the final refinement cycle. The number of reflections so affected ranged in number from 1 to 9 and resulted in negligible shifts in atomic parameters. Low-intensity reflections, $F_o < 3\sigma(F_o)$, were not included in the refinement. Final R factors for all reflections and unrejected reflections are listed in Table 1.

The results of the refinements of the structures of all three polymorphs at the various temperatures are given as follows: cell dimensions in Table 2, strain components of thermal expansion in Table 3, atomic positions and anisotropic temperature factors in

Table 1. Sillimanite, andalusite, and kyanite: number of reflections measured and *R* factors

Temp. (°C)	All Refl.		Unrej.		# Refl.	Low I rej.	$[F_o-F_c]>5$ rej.
	R_w	R	R_w	R			
Sillimanite							
25	0.043	0.041	0.033	0.032	659	120	2
400	0.044	0.046	0.035	0.035	660	137	2
600	0.039	0.045	0.033	0.033	661	150	1
800	0.037	0.045	0.031	0.032	662	163	1
1000	0.056	0.050	0.037	0.035	663	174	2
Andalusite							
25	0.063	0.035	0.031	0.028	682	62	5
400	0.055	0.035	0.029	0.027	685	77	4
600	0.061	0.039	0.032	0.029	686	70	6
800	0.078	0.039	0.031	0.029	688	87	4
1000	0.060	0.041	0.036	0.031	690	88	4
Kyanite							
25	0.044	0.040	0.036	0.033	2140	248	7
400	0.044	0.037	0.034	0.031	1733	192	9
600	0.051	0.043	0.040	0.036	1741	214	8

Table 3. Sillimanite, andalusite, and kyanite: principal strain components of thermal expansion (with standard deviations in parentheses)

Variable Range	Principal Strain Components per 1°C ($\times 10^{-5}$)	Orientation of Principal Axes: Angle (degrees) with respect to: +a	+b	+c
Kyanite				
25→400°C	1.22(7)	108(5)	79(6)	12(4)
	0.77(6)	66(9)	40(8)	96(7)
	0.48(5)	31(7)	127(8)	80(4)
25→600°C	1.20(4)	112(5)	77(4)	15(3)
	0.83(4)	47(7)	61(7)	89(6)
	0.57(3)	129(5)	32(6)	105(3)
25→800°C	1.10(3)	109(5)	76(3)	15(3)
	0.81(3)	40(6)	68(6)	91(5)
	0.60(2)	123(5)	27(5)	105(3)
Sillimanite				
25→800°C	0.66	90	0	90
	0.40	90	90	0
	0.16	0	90	90
Andalusite				
25→800°C	1.29	0	90	90
	0.87	90	0	90
	0.23	90	90	0

Table 4, axes of atomic thermal ellipsoids and isotropic equivalent temperature factors in Table 5[1], Si–O and Al–O interatomic distances and angles in Tables 6 and 7[1] respectively. Room-temperature refinements both preceding and following high-temperature analysis were conducted and found to match within $\pm 2\sigma$ for all parameters. Only the initial analysis is included in the tables. The room-temperature atomic positions of andalusite and sillimanite agree

[1] To receive a copy of Tables 5, 7, 10, order Document AM-79-096 from the Business Office, Mineralogical Society of America, 2000 Florida Ave., N.W., Washington, D.C. 20009. Please remit $1.00 in advance for the microfiche.

Table 2. Sillimanite, andalusite, and kyanite: cell dimensions as a function of temperature (with standard deviations in parentheses)

	25°C	400°C	600°C	800°C	1000°C
Sillimanite					
a (Å)	7.4883(7)	7.4932(9)	7.4967(8)	7.4998(8)	7.5035(8)
b (Å)	7.6808(7)	7.7035(9)	7.7136(8)	7.7255(8)	7.7387(8)
c (Å)	5.7774(5)	5.7872(5)	5.7921(6)	5.7978(6)	5.8040(6)
V (Å^3)	332.29(5)	334.06(6)	334.94(6)	335.92(6)	337.02(6)
(cm^3/mol)	50.049(7)	50.315(9)	50.448(9)	50.595(9)	50.761(9)
Andalusite					
a (Å)	7.7980(7)	7.8355(13)	7.8556(14)	7.8759(14)	7.8976(16)
b (Å)	7.9031(10)	7.9289(18)	7.9424(18)	7.9567(18)	7.9735(20)
c (Å)	5.5566(5)	5.5611(10)	5.5642(10)	5.5664(10)	5.5695(11)
V (Å^3)	342.45(6)	345.50(11)	347.17(11)	348.82(11)	350.72(13)
(cm^3/mol)	51.58(1)	52.04(2)	52.29(2)	52.54(2)	52.82(2)
Kyanite					
a (Å)	7.1262(12)	7.1423(8)	7.1582(9)	7.1687(9)	
b (Å)	7.8520(10)	7.8724(10)	7.8821(11)	7.8917(11)	
c (Å)	5.5724(10)	5.5968(6)	5.6089(6)	5.6182(6)	
α (°)	89.99(2)	89.94(1)	89.90(1)	89.89(1)	
β (°)	101.11(2)	101.18(1)	101.21(1)	101.20(1)	
γ (°)	106.03(1)	105.99(1)	105.98(1)	105.98(1)	
V (Å^3)	293.60(9)	296.31(7)	297.99(7)	299.29(7)	
(cm^3/mol)	44.22(1)	44.63(1)	44.88(1)	45.08(1)	

Table 4. Sillimanite, andalusite, and kyanite: atomic positional coordinates and anisotropic temperature factors as a function of temperature (with standard deviations in parentheses)

		25°C	400°C	600°C	800°C	1000°C
Sillimanite						
Al_1	x	0	0	0	0	0
	y	0	0	0	0	0
	z	0	0	0	0	0
	β_{11}	0.0009(1)	0.0024(1)	0.0031(1)	0.0040(1)	0.0050(2)
	β_{22}	0.0019(1)	0.0036(1)	0.0043(1)	0.0053(1)	0.0062(2)
	β_{33}	0.0041(2)	0.0061(2)	0.0068(2)	0.0079(2)	0.0090(3)
	β_{12}	-0.0001(1)	-0.0001(1)	0.0000(1)	0.0000(1)	0.0000(1)
	β_{13}	0.0000(2)	-0.0002(2)	-0.0001(2)	-0.0002(2)	-0.0002(3)
	β_{23}	-0.0001(2)	-0.0001(2)	-0.0001(2)	-0.0001(2)	-0.0002(3)
Al_2	x	0.1417(1)	0.1415(1)	0.1414(2)	0.1412(2)	0.1410(2)
	y	0.3449(1)	0.3455(2)	0.3459(2)	0.3461(2)	0.3463(2)
	z	0.25	0.25	0.25	0.25	0.25
	β_{11}	0.0012(2)	0.0026(2)	0.0034(2)	0.0043(2)	0.0052(3)
	β_{22}	0.0024(1)	0.0038(2)	0.0045(2)	0.0054(2)	0.0065(2)
	β_{33}	0.0045(3)	0.0067(3)	0.0074(3)	0.0085(3)	0.0096(4)
	β_{12}	-0.0001(1)	-0.0001(2)	-0.0002(2)	-0.0003(2)	-0.0003(2)
	β_{13}	0	0	0	0	0
	β_{23}	0	0	0	0	0
Si	x	0.1533(1)	0.1528(1)	0.1525(1)	0.1523(1)	0.1520(2)
	y	0.3402(1)	0.3407(1)	0.3408(1)	0.3410(1)	0.3413(2)
	z	0.75	0.75	0.75	0.75	0.75
	β_{11}	0.0008(1)	0.0024(2)	0.0030(2)	0.0037(2)	0.0044(2)
	β_{22}	0.0019(1)	0.0032(1)	0.0040(2)	0.0047(2)	0.0057(2)
	β_{33}	0.0045(2)	0.0062(3)	0.0067(3)	0.0080(3)	0.0088(3)
	β_{12}	-0.0002(1)	-0.0004(1)	-0.0005(1)	-0.0006(2)	-0.0007(2)
	β_{13}	0	0	0	0	0
	β_{23}	0	0	0	0	0
O_A	x	0.3605(3)	0.3598(3)	0.3597(4)	0.3594(4)	0.3596(4)
	y	0.4094(3)	0.4099(4)	0.4100(4)	0.4100(4)	0.4106(5)
	z	0.75	0.75	0.75	0.75	0.75
	β_{11}	0.0012(3)	0.0024(4)	0.0033(4)	0.0040(5)	0.0052(6)
	β_{22}	0.0027(3)	0.0051(4)	0.0063(5)	0.0072(5)	0.0083(6)
	β_{33}	0.0055(6)	0.0081(7)	0.0084(7)	0.0107(8)	0.0117(9)
	β_{12}	-0.0005(3)	-0.0010(3)	-0.0016(4)	-0.0019(4)	-0.0024(5)
	β_{13}	0	0	0	0	0
	β_{23}	0	0	0	0	0
O_B	x	0.3569(3)	0.3567(3)	0.3568(3)	0.3570(4)	0.3566(5)
	y	0.4341(3)	0.4351(4)	0.4349(4)	0.4352(4)	0.4363(5)
	z	0.25	0.25	0.25	0.25	0.25
	β_{11}	0.0012(3)	0.0027(4)	0.0033(4)	0.0040(4)	0.0051(5)
	β_{22}	0.0033(4)	0.0053(4)	0.0062(4)	0.0073(4)	0.0095(6)
	β_{33}	0.0047(6)	0.0076(6)	0.0086(7)	0.0100(7)	0.0102(9)
	β_{12}	-0.0004(3)	-0.0012(3)	-0.0012(4)	-0.0017(4)	-0.0021(5)
	β_{13}	0	0	0	0	0
	β_{23}	0	0	0	0	0
O_C	x	0.4763(3)	0.4771(4)	0.4771(5)	0.4777(5)	0.4783(6)
	y	0.0015(4)	0.0012(5)	0.0013(5)	0.0005(5)	0.0006(6)
	z	0.75	0.75	0.75	0.75	0.75
	β_{11}	0.0030(4)	0.0068(6)	0.0081(6)	0.0103(7)	0.0129(9)
	β_{22}	0.0033(3)	0.0070(4)	0.0080(4)	0.0099(5)	0.0112(6)
	β_{33}	0.0089(6)	0.0154(8)	0.0183(9)	0.0215(10)	0.0250(12)
	β_{12}	-0.0016(3)	-0.0036(3)	-0.0047(4)	-0.0057(5)	-0.0072(6)
	β_{13}	0	0	0	0	0
	β_{23}	0	0	0	0	0
O_D	x	0.1252(2)	0.1249(2)	0.1247(2)	0.1247(2)	0.1248(3)
	y	0.2230(2)	0.2241(2)	0.2245(2)	0.2250(2)	0.2249(2)
	z	0.5145(3)	0.5146(4)	0.5142(4)	0.5145(4)	0.5142(4)
	β_{11}	0.0022(2)	0.0051(2)	0.0061(3)	0.0078(3)	0.0091(4)
	β_{22}	0.0025(2)	0.0039(2)	0.0048(2)	0.0056(2)	0.0062(3)
	β_{33}	0.0044(4)	0.0065(4)	0.0073(4)	0.0083(4)	0.0094(5)
	β_{12}	-0.0005(2)	-0.0012(2)	-0.0016(2)	-0.0019(2)	-0.0022(3)
	β_{13}	0.0000(3)	-0.0002(3)	-0.0003(4)	-0.0004(4)	-0.0006(5)
	β_{23}	0.0000(3)	-0.0002(3)	0.0000(3)	-0.0002(3)	-0.0001(4)
Andalusite						
Al_1	x	0	0	0	0	0
	y	0	0	0	0	0
	z	0.2419(1)	0.2419(1)	0.2419(1)	0.2420(2)	0.2418(2)
	β_{11}	0.0021(1)	0.0052(1)	0.0069(1)	0.0086(1)	0.0107(2)
	β_{22}	0.0029(1)	0.0046(1)	0.0056(1)	0.0067(1)	0.0077(1)
	β_{33}	0.0023(2)	0.0040(2)	0.0049(2)	0.0059(2)	0.0070(3)
	β_{12}	0.0005(1)	0.0015(1)	0.0021(1)	0.0027(1)	0.0036(1)
	β_{13}	0	0	0	0	0
	β_{23}	0	0	0	0	0
Al_2	x	0.3705(1)	0.3713(1)	0.3718(1)	0.3721(1)	0.3724(1)
	y	0.1391(1)	0.1396(1)	0.1398(1)	0.1401(1)	0.1404(1)
	z	0.5	0.5	0.5	0.5	0.5
	β_{11}	0.0009(1)	0.0021(1)	0.0027(1)	0.0033(1)	0.0042(1)
	β_{22}	0.0026(1)	0.0037(1)	0.0045(1)	0.0050(1)	0.0059(1)
	β_{33}	0.0028(2)	0.0054(1)	0.0065(2)	0.0079(2)	0.0090(2)
	β_{12}	0.0000(1)	-0.0001(1)	-0.0002(1)	-0.0001(1)	0.0001(1)
	β_{13}	0	0	0	0	0
	β_{23}	0	0	0	0	0
O_B	x	0.4246(2)	0.4239(2)	0.4236(2)	0.4231(2)	0.4224(3)
	y	0.3629(2)	0.3641(2)	0.3646(3)	0.3650(3)	0.3661(3)
	z	0	0	0	0	0
	β_{11}	0.0011(2)	0.0026(2)	0.0035(2)	0.0041(2)	0.0055(3)
	β_{22}	0.0031(2)	0.0045(2)	0.0055(3)	0.0068(3)	0.0074(3)
	β_{33}	0.0031(4)	0.0057(4)	0.0067(5)	0.0077(5)	0.0093(6)
	β_{12}	-0.0006(2)	-0.0009(2)	-0.0012(2)	-0.0015(2)	-0.0019(3)
	β_{13}	0	0	0	0	0
	β_{23}	0	0	0	0	0
O_C	x	0.1030(2)	0.1032(2)	0.1031(3)	0.1034(3)	0.1033(3)
	y	0.4003(2)	0.4004(2)	0.4008(3)	0.4009(3)	0.4006(3)
	z	0	0	0	0	0
	β_{11}	0.0010(2)	0.0023(2)	0.0032(3)	0.0032(2)	0.0041(3)
	β_{22}	0.0027(2)	0.0039(2)	0.0044(3)	0.0047(3)	0.0053(3)
	β_{33}	0.0086(5)	0.0163(6)	0.0215(7)	0.0257(8)	0.0306(10)
	β_{12}	0.0002(2)	0.0002(2)	0.0004(2)	0.0004(2)	0.0006(3)
	β_{13}	0	0	0	0	0
	β_{23}	0	0	0	0	0

with the data of Burnham and Buerger (1961) and Burnham (1963a) as well as those of Finger and Prince (1972) within $\pm 2\sigma$. The kyanite atomic positions show somewhat poorer agreement with the data of Burnham (1963b), but within 3σ nonetheless. The temperature factors in this study, as a rule, are considerably larger than those of Burnham and Buerger (1961) and Burnham (1963a,b), most likely due to the neglect of the absorption correction. The volumes and distortions of the Al–O and Si–O polyhedra are given in Table 8, and the observed and calculated structure factors are compared in Table 10[1].

Table 4. (continued)

		25°C	400°C	600°C	800°C	1000°C
Si	x	0.2460(1)	0.2461(1)	0.2462(1)	0.2463(1)	0.2461(1)
	y	0.2520(1)	0.2534(1)	0.2541(1)	0.2547(1)	0.2551(1)
	z	0	0	0	0	0
	β_{11}	0.0007(1)	0.0020(1)	0.0026(1)	0.0033(1)	0.0042(1)
	β_{22}	0.0024(1)	0.0033(1)	0.0039(1)	0.0043(1)	0.0049(1)
	β_{33}	0.0025(2)	0.0046(2)	0.0057(2)	0.0068(2)	0.0080(2)
	β_{12}	0.0000(1)	0.0000(1)	0.0001(1)	010001(1)	0.0000(1)
	β_{13}	0	0	0	0	0
	β_{23}	0	0	0	0	0
O_A	x	0.4233(2)	0.4243(2)	0.4249(2)	0.4256(3)	0.4259(3)
	y	0.3629(2)	0.3629(2)	0.3630(3)	0.3631(3)	0.3629(3)
	z	0.5	0.5	0.5	0.5	0.5
	β_{11}	0.0018(2)	0.0040(2)	0.0048(3)	0.0061(3)	0.0073(3)
	β_{22}	0.0028(2)	0.0038(2)	0.0045(2)	0.0050(2)	0.0058(3)
	β_{33}	0.0030(4)	0.0055(4)	0.0070(5)	0.0081(5)	0.0098(6)
	β_{12}	-0.0003(2)	-0.0006(2)	-0.0009(2)	-0.0010(2)	-0.0014(3)
	β_{13}	0	0	0	0	0
	β_{23}	0	0	0	0	0
O_D	x	0.2305(2)	0.2320(2)	0.2329(2)	0.2335(2)	0.2345(2)
	y	0.1339(2)	0.1356(2)	0.1364(2)	0.1371(2)	0.1379(2)
	z	0.2394(2)	0.2392(2)	0.2392(3)	0.2390(3)	0.2387(3)
	β_{11}	0.0016(2)	0.0038(2)	0.0049(2)	0.0060(2)	0.0072(2)
	β_{22}	0.0032(2)	0.0052(2)	0.0063(2)	0.0071(2)	0.0081(2)
	β_{33}	0.0030(3)	0.0058(3)	0.0072(4)	0.0086(4)	0.0102(5)
	β_{12}	-0.0004(1)	-0.0008(1)	-0.0011(2)	-0.0012(2)	-0.0018(2)
	β_{13}	-0.0004(1)	-0.0011(2)	-0.0015(2)	-0.0017(2)	-0.0023(3)
	β_{23}	0.0005(2)	0.0011(2)	0.0014(2)	0.0018(2)	0.0020(3)

Kyanite		25°C	400°C	600°C
Al_1	x	0.3254(1)	0.3259(1)	0.3263(1)
	y	0.7040(1)	0.7041(1)	0.7042(1)
	z	0.4582(1)	0.4584(1)	0.4586(2)
	β_{11}	0.0013(1)	0.0028(1)	0.0040(2)
	β_{22}	0.0020(1)	0.0041(1)	0.0055(1)
	β_{33}	0.0043(2)	0.0062(2)	0.0084(4)
	β_{12}	0.0007(1)	0.0011(1)	0.0018(1)
	β_{13}	-0.0005(1)	-0.0003(1)	-0.0005(1)
	β_{23}	0.0001(1)	0.0005(1)	0.0008(1)
Al_2	x	0.2974(1)	0.2976(1)	0.2978(1)
	y	0.6989(1)	0.6990(1)	0.6990(1)
	z	0.9505(1)	0.9505(1)	0.9507(2)
	β_{11}	0.0019(1)	0.0040(1)	0.0055(2)
	β_{22}	0.0016(1)	0.0030(1)	0.0040(1)
	β_{33}	0.0045(2)	0.0063(2)	0.0087(2)
	β_{12}	0.0009(1)	0.0016(1)	0.0022(1)
	β_{13}	-0.0005(1)	-0.0002(1)	-0.0003(2)
	β_{23}	-0.0003(1)	-0.0002(1)	-0.0001(1)
Al_3	x	0.0998(1)	0.1000(1)	0.1001(1)
	y	0.3862(1)	0.3859(1)	0.3858(1)
	z	0.6403(1)	0.6403(1)	0.6405(2)
	β_{11}	0.0017(1)	0.0036(1)	0.0048(2)
	β_{22}	0.0015(1)	0.0026(1)	0.0035(1)
	β_{33}	0.0050(2)	0.0081(2)	0.0110(2)
	β_{12}	0.0008(1)	0.0013(1)	0.0019(1)
	β_{13}	-0.0004(1)	0.0001(1)	0.0002(2)
	β_{23}	0.0000(1)	0.0005(1)	0.0006(1)
Al_4	x	0.1120(1)	0.1127(1)	0.1131(1)
	y	0.9175(1)	0.9181(1)	0.9185(1)
	z	0.1649(1)	0.1655(1)	0.1659(2)
	β_{11}	0.0018(1)	0.0037(1)	0.0051(2)
	β_{22}	0.0015(1)	0.0027(1)	0.0036(1)
	β_{33}	0.0050(2)	0.0079(2)	0.0105(2)
	β_{12}	0.0008(1)	0.0016(1)	0.0024(1)
	β_{13}	-0.0004(1)	0.0000(1)	0.0001(1)
	β_{23}	0.0002(1)	0.0007(1)	0.0010(1)
O_A	x	0.1095(2)	0.1100(2)	0.1101(3)
	y	0.1468(2)	0.1466(2)	0.1469(3)
	z	0.1288(3)	0.1292(3)	0.1291(4)
	β_{11}	0.0022(3)	0.0039(3)	0.0049(4)
	β_{22}	0.0017(2)	0.0028(3)	0.0034(3)
	β_{33}	0.0060(4)	0.0094(4)	0.0129(6)
	β_{12}	0.0007(2)	0.0008(2)	0.0013(2)
	β_{13}	-0.0007(3)	-0.0008(3)	-0.0009(4)
	β_{23}	-0.0002(2)	0.0001(3)	0.0002(3)
O_B	x	0.1230(2)	0.1237(2)	0.1239(3)
	y	0.6856(2)	0.6862(2)	0.6868(3)
	z	0.1812(3)	0.1819(3)	0.1817(4)
	β_{11}	0.0018(2)	0.0035(2)	0.0047(3)
	β_{22}	0.0018(2)	0.0030(2)	0.0037(3)
	β_{33}	0.0044(4)	0.0068(4)	0.0089(5)
	β_{12}	0.0006(2)	0.0013(2)	0.0018(3)
	β_{13}	-0.0006(2)	-0.0002(3)	-0.0004(4)
	β_{23}	0.0001(2)	0.0003(3)	0.0003(3)
O_C	x	0.2747(2)	0.2745(2)	0.2744(3)
	y	0.4545(2)	0.4546(2)	0.4542(3)
	z	0.9547(3)	0.9557(3)	0.9560(4)
	β_{11}	0.0024(3)	0.0048(3)	0.0063(4)
	β_{22}	0.0020(2)	0.0033(3)	0.0041(3)
	β_{33}	0.0051(4)	0.0080(5)	0.0100(6)
	β_{12}	0.0008(2)	0.0015(2)	0.0020(3)
	β_{13}	-0.0005(3)	-0.0006(3)	-0.0005(4)
	β_{23}	0.0001(2)	0.0010(3)	0.0006(3)
O_D	x	0.2831(2)	0.2828(3)	0.2830(3)
	y	0.9354(2)	0.9353(2)	0.9358(3)
	z	0.9353(3)	0.9345(3)	0.9341(4)
	β_{11}	0.0026(3)	0.0048(3)	0.0065(4)
	β_{22}	0.0017(2)	0.0033(3)	0.0040(3)
	β_{33}	0.0054(4)	0.0086(5)	0.0111(6)
	β_{12}	0.0010(2)	0.0019(2)	0.0024(3)
	β_{13}	0.0001(3)	0.0008(3)	0.0014(4)
	β_{23}	0.0005(2)	0.0016(3)	0.0015(3)
O_F	x	0.1219(2)	0.1227(2)	0.1229(3)
	y	0.6307(2)	0.6300(2)	0.6300(3)
	z	0.6389(3)	0.6388(3)	0.6396(4)
	β_{11}	0.0019(2)	0.0034(3)	0.0046(4)
	β_{22}	0.0019(2)	0.0031(3)	0.0041(3)
	β_{33}	0.0048(4)	0.0067(5)	0.0090(6)
	β_{12}	0.0007(2)	0.0014(2)	0.0017(3)
	β_{13}	-0.0009(2)	-0.0004(3)	-0.0004(4)
	β_{23}	-0.0005(2)	-0.0002(3)	0.0000(3)
O_G	x	0.2822(2)	0.2819(3)	0.2814(3)
	y	0.4453(2)	0.4443(2)	0.4438(3)
	z	0.4288(3)	0.4281(3)	0.4280(4)
	β_{11}	0.0027(3)	0.0047(3)	0.0062(4)
	β_{22}	0.0019(2)	0.0037(2)	0.0046(3)
	β_{33}	0.0054(4)	0.0084(5)	0.0113(6)
	β_{12}	0.0009(2)	0.0017(2)	0.0021(3)
	β_{13}	-0.0002(3)	0.0008(3)	0.0013(4)
	β_{23}	-0.0002(2)	-0.0001(3)	-0.0006(3)
O_H	x	0.2915(2)	0.2915(3)	0.2916(3)
	y	0.9467(2)	0.9479(2)	0.9483(3)
	z	0.4659(3)	0.4665(3)	0.4670(4)
	β_{11}	0.0026(3)	0.0046(3)	0.0064(4)
	β_{22}	0.0023(2)	0.0040(3)	0.0052(3)
	β_{33}	0.0047(4)	0.0072(5)	0.0092(6)
	β_{12}	0.0013(2)	0.0019(2)	0.0026(3)
	β_{13}	-0.0003(3)	-0.0005(3)	-0.0004(4)
	β_{23}	-0.0002(2)	-0.0008(3)	-0.0011(3)
O_K	x	0.5008(2)	0.5004(2)	0.5004(3)
	y	0.2749(2)	0.2755(3)	0.2755(3)
	z	0.2440(3)	0.2445(3)	0.2443(3)
	β_{11}	0.0023(3)	0.0042(3)	0.0050(4)
	β_{22}	0.0022(2)	0.0043(2)	0.0054(3)
	β_{33}	0.0051(4)	0.0075(5)	0.0099(6)
	β_{12}	0.0013(2)	0.0023(2)	0.0029(3)
	β_{13}	-0.0005(3)	-0.0001(3)	-0.0001(4)
	β_{23}	0.0001(2)	0.0005(3)	0.0005(3)

Results

Unit-cell parameters

Unit-cell parameters of andalusite, sillimanite, and kyanite vary linearly as a function of temperature (Figs. 1–4). Although the room-temperature data of Skinner *et al.* (1961) based on powder-diffraction data agree with those of the present study within 3σ, significant deviations in the high-temperature data are obvious, as shown in Figures 1–4. Since the high-temperature data of Skinner *et al.* (1961) are based on only 4, 4, and 6 independently-measured d values for andalusite, sillimanite, and kyanite respectively, and no estimated errors are given, it is possible that the discrepancies in cell dimensions at elevated temper-

Table 4. (continued)

		25°C	400°C	600°C
Si_1	x	0.2962(1)	0.2961(1)	0.2961(1)
	y	0.0649(1)	0.0651(1)	0.0650(1)
	z	0.7066(1)	0.7068(1)	0.7068(1)
	β_{11}	0.0012(1)	0.0023(1)	0.0033(1)
	β_{22}	0.0013(1)	0.0023(1)	0.0030(1)
	β_{33}	0.0044(1)	0.0065(2)	0.0086(2)
	β_{12}	0.0007(1)	0.0010(1)	0.0016(1)
	β_{13}	-0.0004(1)	-0.0002(1)	-0.0002(1)
	β_{23}	0.0000(1)	-0.0001(1)	0.0001(1)
Si_2	x	0.2910(1)	0.2909(1)	0.2908(1)
	y	0.3317(1)	0.3315(1)	0.3314(1)
	z	0.1892(1)	0.1892(1)	0.1893(1)
	β_{11}	0.0011(1)	0.0025(1)	0.0035(1)
	β_{22}	0.0014(1)	0.0023(1)	0.0030(1)
	β_{33}	0.0040(1)	0.0060(2)	0.0081(2)
	β_{12}	0.0007(1)	0.0011(1)	0.0017(1)
	β_{13}	-0.0007(1)	-0.0006(1)	-0.0007(1)
	β_{23}	-0.0001(1)	-0.0002(1)	-0.0001(1)
O_E	x	0.1084(2)	0.1090(2)	0.1090(3)
	y	0.1520(2)	0.1523(2)	0.1524(3)
	z	0.6669(3)	0.6673(3)	0.6673(4)
	β_{11}	0.0025(3)	0.0041(3)	0.0052(4)
	β_{22}	0.0019(2)	0.0036(3)	0.0041(3)
	β_{33}	0.0051(4)	0.0088(5)	0.0123(6)
	β_{12}	0.0011(2)	0.0022(2)	0.0028(3)
	β_{13}	0.0000(2)	0.0006(3)	0.0007(4)
	β_{23}	0.0006(2)	0.0008(3)	0.0010(3)
O_M	x	0.5015(2)	0.5014(2)	0.5011(3)
	y	0.2312(2)	0.2305(2)	0.2303(3)
	z	0.7553(3)	0.7551(3)	0.7550(4)
	β_{11}	0.0020(3)	0.0040(3)	0.0047(4)
	β_{22}	0.0020(2)	0.0034(2)	0.0044(3)
	β_{33}	0.0055(4)	0.0081(5)	0.0108(6)
	β_{12}	0.0006(2)	0.0007(2)	0.0010(3)
	β_{13}	-0.0004(3)	0.0004(3)	0.0000(4)
	β_{23}	-0.0002(2)	0.0001(3)	0.0000(3)

atures fall within the range of uncertainties involved in their measurements.

Since kyanite is triclinic, there are no symmetry restraints on the orientation of the principal axes of the thermal expansion ellipsoid. These ellipsoids have been calculated between 25°C and 400, 600, and 800°C respectively, using the STRAIN program (Ohashi and Finger, 1973), and the magnitude and orientation of the principal axes are given in Table 3. Included is a similar calculation for andalusite and sillimanite between 25 and 800°C, so that the relative magnitudes of thermal expansion for the three polymorphs can be directly compared. A stereogram of the orientations of the ellipsoids for kyanite is shown in Figure 5.

Bond lengths and angles

Octahedral Al–O bond lengths and volumes increase substantially with increasing temperature (Tables 6 and 8). The rate of increase of octahedral bond distances with temperature in a given polyhedron is a function of the distance itself. Shorter bonds have a higher bond strength than longer ones, and therefore increase less with increasing temperature. Distortion of the polyhedral angles and dimensions has been calculated (except for the five-fold Al_2 atom in andalusite) using the program DISTORT of Hamil (1971, private communication) (Table 8). Al–O octahedra are more highly distorted than Al–O or Si–O tetrahedra and tend to become very slightly more so with increasing temperature. These changes are of a magnitude comparable to the calculated standard deviations in bond length; nevertheless, a trend toward increased distortion is evident. Longitudinal strain $[(\Sigma_i|(l_i/l_0)|)$ where l_i is the individual bond length and l_0 is the "ideal" bond length, based on a perfect polyhedron with bond length l_0 having the same volume as the real coordination polyhedron] is higher than shear distortion $[(\Sigma_i|\tan(\theta_i - \theta_0)|)$, where θ_i is the individual O–X–O bond angle and θ_0 is the ideal bond angle, being 90° for an octahedron and 109.5° for a tetrahedron] for a given polyhedron. The increased octahedral distortions in sillimanite and andalusite are probably the result of restrictions imposed on the expansion of Al_1–O_A and Al_1–O_B bonds caused by the shared octahedral edge O_A–O_B. The longer Al_1–O_D bonds in these two minerals are more free to expand. In contrast, tetrahedral bond lengths, volumes, and distortions remain nearly constant, although most bond lengths and volumes increase slightly. Only two tetrahedral bonds, the short Al_2–O_C and Si–O_C bonds in sillimanite, appear to decrease markedly. The Al_2 atom in andalusite is in an unusual five-coordination, which can be considered as a distorted trigonal bipyramid (Figs. 6 and 7). These Al_2 atoms occur in pairs sharing a common polyhedral edge (O_C–O_C). Al_2–Al_2 repulsion results in longer Al_2–O_C bonds and a short O_C–O_C distance. The shorter Al_2–O_A and Al_2–O_D bonds are much like tetrahedral bonds and change very little with increasing temperature, while the longer Al_2–O_C bond exhibits greater elasticity (Figs. 6 and 7).

Discussion

Bond distances

The thermal response of the tetrahedral bond lengths in the aluminum silicates is different from

Table 6. Sillimanite, andalusite, and kyanite: Al–O and Si–O bond lengths (A) as a function of temperature (with standard deviations in parentheses)

	25°C	400°C	600°C	800°C	1000°C
Sillimanite					
Al_1–O_A (X2)	1.913(1)	1.918(2)	1.920(2)	1.923(2)	1.922(2)
–O_B (X2)	1.868(1)	1.870(2)	1.871(2)	1.871(2)	1.872(2)
–O_D (X2)	1.955(1)	1.966(2)	1.970(2)	1.975(2)	1.978(2)
	1.912	1.918	1.920	1.923	1.924
Al_2–O_B	1.751(2)	1.754(3)	1.755(3)	1.759(3)	1.762(3)
–O_C	1.711(3)	1.706(3)	1.705(4)	1.705(4)	1.701(4)
–O_D (X2)	1.796(2)	1.798(2)	1.798(2)	1.801(2)	1.803(2)
	1.763	1.764	1.764	1.767	1.768
Si–O_A	1.641(2)	1.641(3)	1.642(3)	1.642(3)	1.648(3)
–O_C	1.574(3)	1.574(3)	1.573(4)	1.572(4)	1.574(4)
–O_D (X2)	1.645(2)	1.645(2)	1.647(2)	1.646(2)	1.651(2)
	1.627	1.626	1.627	1.627	1.631
Andalusite					
Al_1–O_A (X2)	1.827(3)	1.828(2)	1.828(2)	1.829(1)	1.831(2)
–O_B (X2)	1.891(3)	1.892(2)	1.892(2)	1.893(1)	1.893(2)
–O_D (X2)	2.086(2)	2.112(2)	2.126(2)	2.138(1)	2.154(2)
	1.935	1.944	1.949	1.953	1.959
Al_2–O_A	1.816(4)	1.818(4)	1.821(2)	1.823(2)	1.823(3)
–O_A	1.839(4)	1.845(4)	1.846(2)	1.851(2)	1.853(3)
–O_C	1.899(4)	1.907(4)	1.909(2)	1.913(2)	1.922(3)
–O_C					
–O_D (X2)	1.814(3)	1.816(3)	1.816(2)	1.817(1)	1.818(2)
	1.836	1.840	1.842	1.844	1.847
Si–O_B	1.645(4)	1.646(4)	1.647(2)	1.646(2)	1.650(2)
–O_B	1.618(4)	1.616(4)	1.619(2)	1.619(2)	1.618(3)
–O_C (2X)	1.630(2)	1.629(3)	1.630(2)	1.629(1)	1.628(2)
	1.631	1.630	1.632	1.631	1.631
Kyanite					
Al_1–O_B	1.873(2)	1.877(2)	1.883(2)		
–O_B	1.884(2)	1.889(2)	1.896(2)		
–O_F	1.971(2)	1.984(2)	1.990(2)		
–O_G	1.987(2)	2.003(2)	2.008(2)		
–O_H	1.847(1)	1.849(2)	1.852(2)		
–O_K	1.848(2)	1.853(2)	1.857(2)		
–O_M	1.902	1.909	1.914		
Al_2–O_B	1.938(2)	1.945(2)	1.948(2)		
–O_C	1.881(2)	1.886(2)	1.891(2)		
–O_D	1.889(2)	1.893(2)	1.900(2)		
–O_F	1.913(2)	1.919(2)	1.920(2)		
–O_K	1.930(2)	1.940(2)	1.944(2)		
–O_M	1.925(1)	1.931(2)	1.935(2)		
	1.913	1.919	1.923		
Al_3–O_B	1.986(2)	1.996(2)	2.002(2)		
–O_C	1.923(2)	1.934(2)	1.937(2)		
–O_E	1.862(2)	1.863(2)	1.864(2)		
–O_F	1.882(2)	1.884(2)	1.886(2)		
–O_F	1.968(1)	1.978(2)	1.987(2)		
–O_G	1.884(2)	1.891(2)	1.894(2)		
	1.919	1.924	1.928		
Al_4–O_A	1.816(2)	1.815(2)	1.818(2)		
–O_A	1.997(2)	2.012(2)	2.019(2)		
–O_A	1.846(1)	1.850(2)	1.850(2)		
–O_B	1.910(2)	1.919(2)	1.926(2)		
–O_D	1.933(2)	1.944(2)	1.949(2)		
–O_E	1.875(2)	1.878(2)	1.881(2)		
–O_H	1.896	1.903	1.907		
Si_1–O_D	1.631(2)	1.634(2)	1.631(2)		
–O_E	1.643(2)	1.642(2)	1.646(2)		
–O_H	1.621(2)	1.621(2)	1.621(2)		
–O_M	1.646(2)	1.648(2)	1.649(2)		
	1.635	1.636	1.637		
Si_2–O_A	1.640(2)	1.642(2)	1.642(2)		
–O_C	1.629(2)	1.632(2)	1.632(2)		
–O_G	1.627(2)	1.627(2)	1.629(2)		
–O_K	1.649(1)	1.648(2)	1.651(2)		
	1.636	1.637	1.639		

Table 8. Sillimanite, andalusite, and kyanite: polyhedral volumes and strain as a function of temperature

	25°C	400°C	600°C	800°C	1000°C
Sillimanite					
Al_1 Volume (Å^3)	9.173	9.258	9.292	9.329	9.339
Longit. Strain	0.103	0.111	0.114	0.119	0.119
Shear Strain	0.815	0.821	0.821	0.819	0.849
Total Strain	0.918	0.932	0.935	0.938	0.968
Al_2 Volume	2.787	2.793	2.793	2.805	2.810
Longit. Strain	0.076	0.077	0.077	0.078	0.081
Shear Strain	0.380	0.375	0.380	0.374	0.355
Total Strain	0.455	0.452	0.457	0.453	0.436
Si Volume	2.207	2.204	2.208	2.205	2.223
Longit. Strain	0.062	0.065	0.067	0.068	0.071
Shear Strain	0.156	0.157	0.165	0.159	0.165
Total Strain	0.218	0.222	0.232	0.227	0.236
Andalusite					
Al_1 Volume	9.538	9.666	9.729	9.794	9.878
Longit. Strain	0.303	0.334	0.352	0.365	0.384
Shear Strain	0.635	0.640	0.645	0.647	0.636
Total Strain	0.937	0.974	0.979	1.012	1.020
Al_2 Volume	5.151	5.187	5.197	5.220	5.250
Si Volume	2.212	2.209	2.216	2.213	2.214
Longit. Strain	0.019	0.020	0.018	0.017	0.020
Shear Strain	0.282	0.273	0.268	0.266	0.268
Total Strain	0.301	0.294	0.287	0.283	0.288
Kyanite					
Al_1 Volume	8.973	9.073	9.143		
Longit. Strain	0.148	0.161	0.161		
Shear Strain	1.133	1.149	1.161		
Total Strain	1.281	1.310	1.322		
Al_2 Volume	9.135	9.219	9.277		
Longit. Strain	0.071	0.076	0.072		
Shear Strain	1.133	1.204	1.205		
Total Strain	1.244	1.280	1.277		
Al_3 Volume	9.159	9.247	9.304		
Longit. Strain	0.130	0.140	0.146		
Shear Strain	1.325	1.350	1.351		
Total Strain	1.455	1.490	1.497		
Al_4 Volume	8.917	9.007	9.063		
Longit. Strain	0.160	0.174	0.181		
Shear Strain	1.088	1.105	1.105		
Total Strain	1.247	1.279	1.286		
Si_1 Volume	2.240	2.244	2.246		
Longit. Strain	0.023	0.021	0.026		
Shear Strain	0.177	0.180	0.179		
Total Strain	0.200	0.201	0.205		
Si_2 Volume	2.242	2.246	2.252		
Longit. Strain	0.020	0.019	0.020		
Shear Strain	0.230	0.228	0.220		
Total Strain	0.250	0.247	0.240		

that for low albite (Winter *et al.*, 1977), in which many of the T–O bond lengths appear to decrease with increasing temperature. No corrections for thermal vibrations, following the method of Busing and Levy (1964), have been applied to the bond lengths in the aluminum silicates, since the exact nature of mutual vibration of the individual atom pairs is unknown. The result of thermal vibration is an apparent reduction in calculated interatomic distances. The

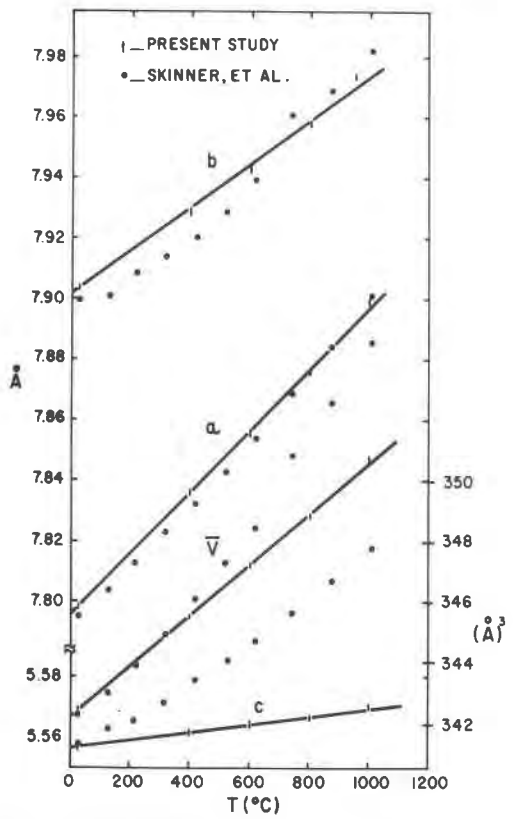

Fig. 1. Andalusite: unit-cell dimensions and volumes as a function of temperature. Error bars represent ±one standard deviation.

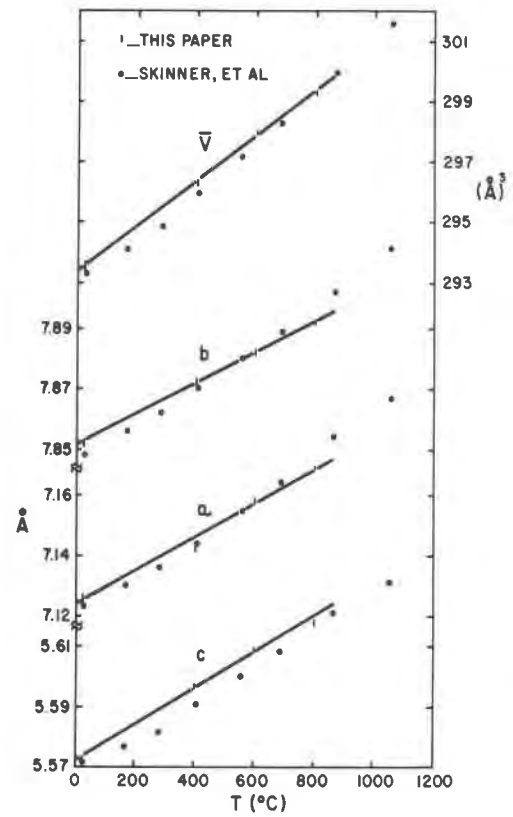

Fig. 3. Kyanite: unit-cell dimensions and volumes as a function of temperature. Error bars represent ±one standard deviation.

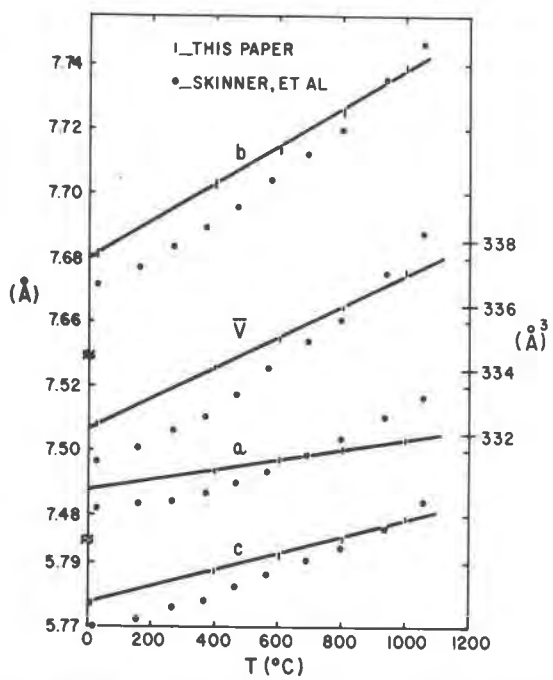

Fig. 2. Sillimanite: unit-cell dimensions and volumes as a function of temperature. Error bars represent ±one standard deviation.

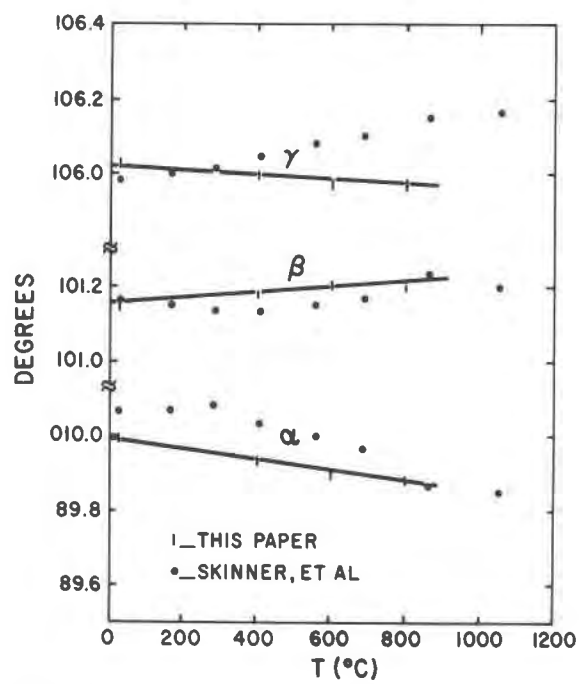

Fig. 4. Kyanite: unit-cell angles as a function of temperature. Error bars represent ±one standard deviation.

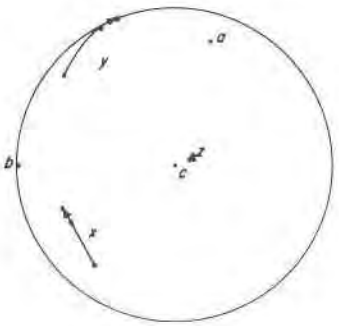

Fig. 5. Kyanite: stereographic projection of the minimum (x), intermediate (y), and maximum (z) axes of the thermal strain ellipsoids for kyanite at 25° → 400°C, 25° → 600°C, and 25° → 800°C respectively in the direction of the arrows. Unit-cell axes are also shown.

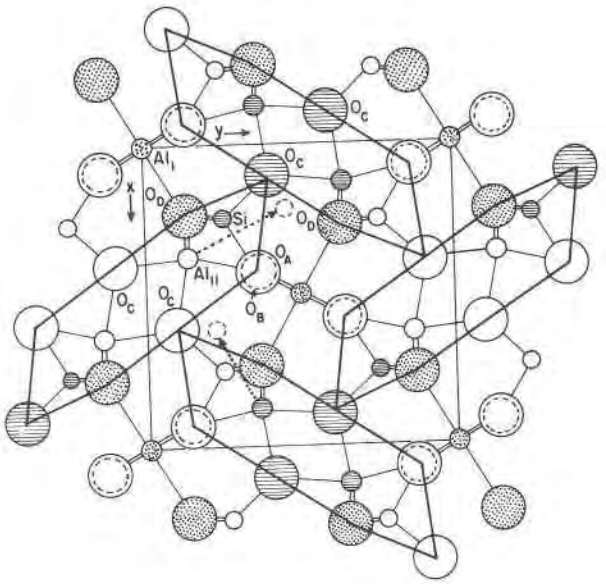

Fig. 6. Projection of the andalusite structure on (001) (after Burnham and Buerger, 1961). Atoms are represented by striped circles at $z = 0$, stippled circles at $z \cong 1/4$, and clear circles at $z = 1/2$. Chains of Si and Al_2 polyhedra are outlined. Dashed circles and arrows show the hypothesized shifts of Al_2 to positions adopted in the kyanite structure.

albite structure permits more freedom of atomic motion, and thus much higher vibrational amplitudes at a given temperature, than does the structure of the aluminum silicate minerals. Therefore, reduction in observed bond lengths due to thermal vibration is greater in albite than in the aluminum silicates at high temperatures, and the uncorrected bond length values appear progressively smaller as the temperature and therefore the magnitude of the correction increases. The lesser vibrational amplitudes in the aluminum silicate minerals (usually less than one-half the value for low albite at a corresponding temperature) is insufficient to decrease the calculated bond lengths enough to overcome the slight thermal expansions of the strong tetrahedral bonds.

As mentioned above, the only tetrahedral bonds in the aluminum silicates which appear to decrease at high temperature are the Al_2–O_C and Si–O_C bonds in sillimanite. If the only cause for an apparent decrease in bond lengths is the thermal vibrations, one would expect large amplitudes of vibration to be associated with these atoms. Indeed, O_C in sillimanite is the only atom in all three polymorphs that is bonded to only two cations instead of three and is thus relatively free to vibrate. The isotropic equivalent temperature factor, B for O_C, is nearly twice that of the other oxygen atoms in all three polymorphs. These results for the aluminum silicates strongly support the contention of Winter *et al.* (1977) that, although tetrahedral Si–O and Al–O bonds in silicates are quite strong and are not subject to large expansions at temperatures up to 1000°C, the apparent contractions in these bond lengths at high temperatures are strictly the result of errors in the calculation of true bond lengths caused by thermal vibration.

Thermal expansion of the unit-cell dimensions

The rigid tetrahedra and more elastic octahedra with pronounced expansion along Al_1–O_D have a profound effect on the characteristics of cell expansion of the aluminum silicate minerals. In andalusite, the a cell dimension expands more than b, which in turn expands much more than c (Fig. 1). Parallel to c are not only chains of octahedra, but also fully extended chains of alternating Si tetrahedra and Al_2 trigonal bipyramids (see Fig. 7). The bonds involved in the latter chains along the c direction vary little

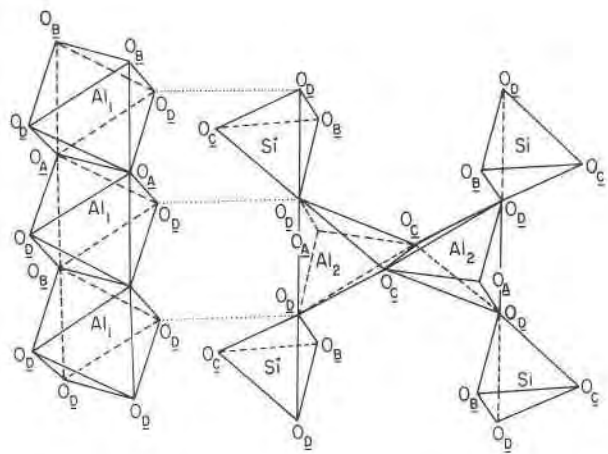

Fig. 7. Andalusite: polyhedral chains parallel to the c axis (after Burnham and Buerger, 1961).

with temperature and thus limit expansion in the *c* direction. Within the *a*–*b* plane, the more elastic Al_1–O_D bond is approximately 30° to either side of the *a* axis (Fig. 6). Thus, the average direction of the large Al_1–O_D expansion is effectively the *a* direction. Therefore the relative magnitudes of axial expansion in andalusite are $a > b > c$.

In sillimanite the elastic Al_1–O_D bond is now 30° to either side of *b* (Fig. 8). Thus, *b* would be expected to expand more than *a*, which is the case. The Al_1–O_A bond in sillimanite is considerably longer than it is in andalusite. This is a result of the Al^{VI}_1–O_A–Si^{IV} linkage in sillimanite *vs.* the Al^{VI}_1–O_A–Al^{V}_2 linkage in andalusite. The Si–O_A bond in sillimanite has a higher bond strength (1.0 valence units; Pauling, 1960) than the Al_2–O_A bond in andalusite (0.6 v.u.). The Al_1–O_A bond in sillimanite is correspondingly weaker, and therefore longer. An opposite though lesser effect for O_B may also be observed. The Si^{IV}–O_B bond in andalusite and Al^{IV}–O_A (as well as Al^{IV}–O_B) bond in sillimanite have bond strengths of 1.0 and 0.75 v.u. respectively. The overall result is a slightly lower Al_1–O_A and Al_1–O_B bond strength in sillimanite than in andalusite. This, in turn, is compensated by a somewhat stronger and shorter Al_1–O_D bond in sillimanite, which expands less with increasing temperature than the same bond in andalusite. The *b* unit-cell axis, which bisects the two possible orientations of these Al_1–O_D bonds, also expands less. In spite of the tetrahedral chains which run parallel to *c* in sillimanite, *c* expands more than *a*. The double chains of Si and Al_2 tetrahedra, which crosslink the octahedral chains (Fig. 9), leave open tunnels parallel to *c* (Fig. 8). These tunnels permit minor rotations of the chains to occur. As temperature increases, the double chains labelled *A* in Figure 8 rotate clockwise and those labelled *B* rotate counterclockwise. This chain rotation facilitates the expansion of the *b* axis and works against the expansion of the *a* axis. In andalusite, this rotation is prevented by Al_2–O_C bonds, which bridge across the tunnels and create a three-dimensional network of Al_2–O–Si polyhedra (Fig. 6).

The orientation of the maximum thermal expansion direction for kyanite is within 12° of *c* (Fig. 5). There are four crystallographically-distinct Al atoms in kyanite. Continuous chains of alternating Al_1 and Al_2 octahedra occur parallel to *c* (Fig. 10). Al_3 and Al_4 occupy octahedral sites adjacent to the chains in a step-like fashion (Fig. 11), in a manner representing a distorted cubic close-packing. These chains are linked by isolated silicate tetrahedra. Since there are no continuous tetrahedral chains parallel to *c* in kyanite,

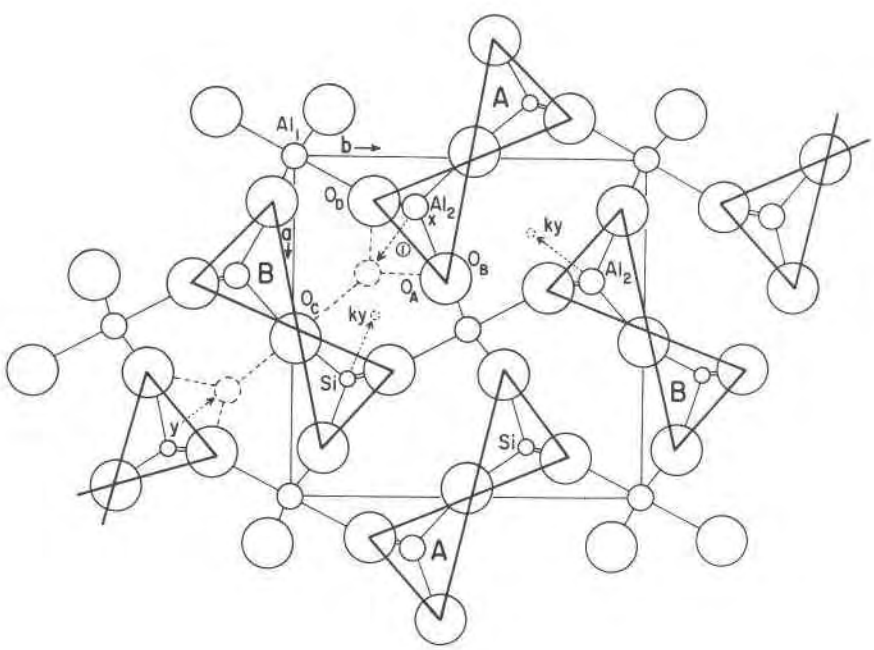

Fig. 8. Sillimanite: partial projection of the structure between $z = 0$ and $z = 1/2$ (after Burnham, 1963a). Tetrahedral chains are outlined. Dashed circles and arrows show the hypothesized shifts of Al_2 atoms for the sillimanite–andalusite and sillimanite–kyanite inversions. Note that one of the shifts for the sillimanite–kyanite inversion appears to involve a Si atom. This actually represents a shift for an Al_2 atom at $z = 3/4$.

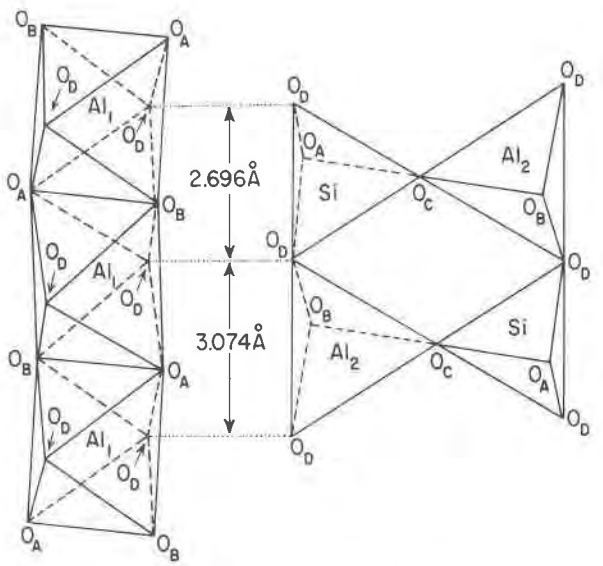

Fig. 9. Sillimanite: polyhedral chains parallel to the *c* axis (after Burnham, 1963a).

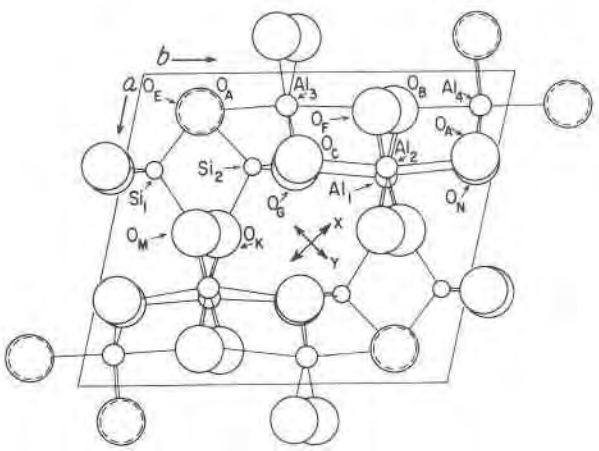

Fig. 10. Kyanite: projection of the structure on (001) (after Burnham, 1963b).

there is no rigid constraint to thermal expansion in this direction. In addition, the complex octahedral chains share several edges (five each for Al_1 and Al_3, four each for Al_2 and Al_4), resulting in no clearly dominant octahedral expansion directions. Therefore, the magnitude of thermal expansion is more uniformly distributed. The rigid silicate tetrahedral edges joining Al_1 and Al_2 octahedra along O_G–O_C and O_H–O_D (Fig. 10) cause rotation about *a* of the Al_1–Al_2 octahedral chains as temperature increases. Other tetrahedral edges linking Al_1–Al_2 octahedral chains to Al_3 and Al_4 *via* O_M–O_A cause similar rotations of Al_3 and Al_4. These rotations decrease the γ angle and result in the $y > x$ expansion shown in Figure 10.

Polymorphic phase transformations

The detailed crystal structures of the three aluminum silicate polymorphs, now available at high temperatures, lead one to speculate on the mechanisms of the polymorphic transformations. The dense tetrahedral Si–Al_2 chains in sillimanite separated by large voids (Fig. 8) are of limited stability, as indicated by the unusual behavior of the O_C atom. With two very short bond distances to Al_2 and Si along one direction and two large voids in the other direction, O_C displays a large amplitude of vibration normal to the Si–O–Al_2 plane. As a result of this uneven distribution of cations, the Al_2 atom (labeled *X* in Fig. 8) is compelled to break the Al_2–O_C bond and bridge the void toward another O_C, as shown by arrow #1 in Figure 8. A second Al atom (an obvious choice is labeled *Y* in Fig. 8) would bridge in like manner, creating the Si–Al–Al–Si chains of andalusite outlined in Figure 6. An O_C atom set free by the previous rupture of an Al_2–O_C bond would migrate 0.5 *c* and be bonded to two joined Al_2 atoms. Unfortunately

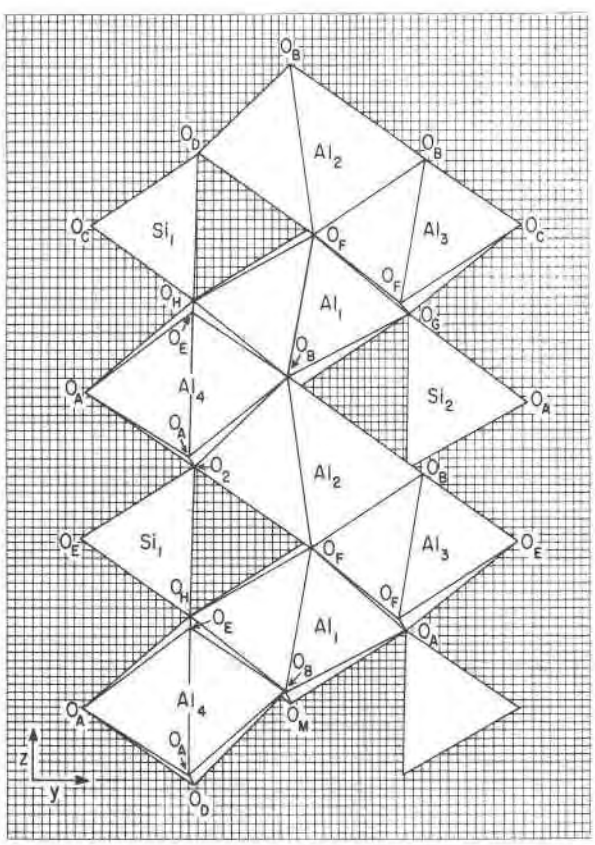

Fig. 11. Kyanite: polyhedral chains parallel to the *c* axis.

for this simple mechanism, one of the Al_2 atoms which shifted (X in Fig. 8) is at $z = 0.25$, while the other (Y) is at $z = 0.75$. Such a mechanism would require diffusion and interchange of half of the Si and Al_2 atoms. Alternative choices of bridging Al_2 shifts encounter the same problem. The diffusion of Si and Al in silicates is a very sluggish process (Al/Si order/disorder reactions in feldspars are quite slow, see *e.g.* McConnell and McKie, 1960). Thus the diffusion required for the andalusite–sillimanite transformation is a major inhibiting factor. Al/Si disorder in sillimanite would greatly facilitate this transformation. Calorimetric data (Navrotsky *et al.*, 1973), heat-treating experiments (Beger *et al.*, 1970), as well as theoretical considerations (Holdaway, 1971; Greenwood, 1972) indicate that some degree of Al/Si disorder occurs in sillimanite.

In andalusite, the unusual five-coordinated Al_2 polyhedron expands very unevenly as temperature increases. The longest Al_2–O_C bond expands at a disproportionately greater rate than the other four Al_2–O bonds (Table 6). Thus, at higher temperatures the five-coordination becomes unstable, and the structure transforms to sillimanite. If the reverse of the previously described mechanism for the sillimanite-to-andalusite transformation were to take place, Si–Al diffusion would not be such an obstacle, and disordered sillimanite would be produced. The resulting sillimanite would have chains of alternating dimers of Si–Si and Al–Al tetrahedra along c. There is no direct evidence yet for such fine domain structure in sillimanite. Perhaps any such domains are quickly destroyed, in accordance with the aluminum avoidance rule.

In an attempt to detect spatial disorder in the Brandywine Springs sample, a linear curve was fitted to the isotropic equivalent temperature factors of each atom *vs.* absolute temperature. Such plots are quite linear in low albite (Quareni and Taylor, 1971; Winter *et al.*, 1977) and should extrapolate to $B = 0$ at 0°K, where thermal motion ceases. Curiously, all such extrapolations for the aluminum silicates result in small positive values of B at 0°K, indicating a small degree of spatial disorder. The average values of B extrapolated to 0° K are 0.159, 0.156, and 0.246 for andalusite, kyanite, and sillimanite respectively. The values of B for andalusite and kyanite are within 3σ of 0 at 0° K, whereas many of the sillimanite B values are not, indicating some Al/Si disorder. Perhaps a structure determination of a sillimanite grain coherently replacing an andalusite grain would exhibit the type of disorder mentioned here.

In aluminosilicates increasing pressure favors octahedrally-coordinated Al, as it requires less volume. In the sillimanite→kyanite transformation, the tetrahedral Al_2 in sillimanite shifts into adjacent octahedral positions (Al_3 and Al_4 in Fig. 10). This requires the breaking of the Al_2–O_B bond in sillimanite (Fig. 8) and the formation of Al_4–O_B, Al_4–O_A, and Al_4–O_C bonds in kyanite (a similar mechanism exists for Al_2(sill)→Al_3(ky), Fig. 10). Rotation of the octahedral chains must also occur, but no major Si/Al diffusion is required as in the andalusite–sillimanite transition. A similar mechanism can be proposed for the andalusite→kyanite transition only using different Al_2 pairs to join a given Al_1 chain (see arrows in Fig. 6), thereby also avoiding the necessity of Al/Si diffusive interchange.

The polymorphic transformations of the aluminum silicate minerals are major reconstructive transformations, involving the breakage and formation of several bonds, as well as rotation of the octahedral chains. In addition, the andalusite–sillimanite transformation requires diffusive interchange of half of the Al_2 and Si atoms. In the light of this fact and the small changes in thermodynamic properties associated with these transformations, it is not surprising that metastable coexistence of these polymorphs is so common. It is also understandable that among the numerous reported occurrences of two or three coexisting polymorphs, the crystallographically incoherent transformation is far more common than the coherent transformation/replacement (see Pitcher, 1965, for a review of the occurrences prior to that date; also Hietanen, 1956; Woodland, 1963; Kwak, 1971). Among the few described coherent replacement textures, the andalusite↔kyanite and sillimanite↔kyanite transitions are much more common than the andalusite↔sillimanite transition. This is to be expected, considering the Al–Si diffusion necessary for the latter transformation. Of the few reported replacement textures involving andalusite and sillimanite (Hietanen, 1956; Kwak, 1971), the andalusite→sillimanite transition is the more commonly observed, which may be a result of the possible andalusite→domain sillimanite transition and the more difficult ordered-sillimanite→andalusite transition mechanisms. An alternative explanation is that the andalusite→sillimanite transition is a prograde reaction, whereas the sillimanite→andalusite transition is a characteristically more sluggish retrograde reaction, except in cases where a low-pressure late-thermal event overprints an earlier regional event (*e.g.* Idaho Batholith, Hietanen, 1956).

The aluminum silicate phase relations

It is hoped that the new volume–temperature data will improve the compatibility of the molar volumes and $(\partial V/\partial T)_P$ curves with experimentally-derived data for the aluminum silicate minerals. The slopes and intercepts of the volume/temperature data based on linear fits are given in Table 9. The ΔV of reaction for the polymorphic inversions at T^{eq} and one atm can thus be calculated. Compressibility corrections can be neglected, since these corrections are negligible below five kbar, and the uncertainties in the compressibility data are large (Brace *et al.*, 1969).

Although there is little agreement among the various investigators on the location of the triple point (see Zen, 1969, for a review), we accept the determination of Holdaway (1971) at 510°C and 3.76 kbar as the most reliable, which is also preferred by Anderson *et al.* (1977) on the basis of thermodynamic consistency. In combination with the one atm data of Weill (1966), Holdaway chose a one atm intercept for the andalusite–sillimanite reaction of 770°C. The resulting dP/dT slope for the reaction is -13.97 bars/degree. The average ΔH of solution for sillimanite (corrected for Fe content), measured by the calorimeter at 700°C, is 6.88±0.11 kcal/mol (Anderson and Kleppa, 1969), while the corresponding value for andalusite is 7.55±0.21 kcal/mol (Anderson *et al.*, 1977). The resulting ΔH_r is 670±230 cal/mol. Using the Clapeyron equation, the ΔV of the present study can be compared with that of Skinner *et al.* (1961) by calculating the corresponding ΔH from the known slope and T and comparing these enthalpies with that derived calorimetrically. The ΔV of Skinner *et al.* (1961) results in a ΔH of 800 cal/mol (assuming $\partial \Delta H/\partial T = 0$ between 700 and 770°C), while our ΔV results in a ΔH of 670 cal/mol. Although both values agree with the calorimetric results within error limits, the present volume data give a better fit. This agreement in enthalpy values requires that the ΔS of Al/Si disorder in sillimanite be the same in the experimental and calorimetric samples (or both zero). Similar calculations of ΔH_r for the kyanite–andalusite and the sillimanite–kyanite reactions based on the two molar volume data sets are compared with those calculated from the calorimetric data using the heat capacity equations of Pankratz and Kelley (1964) as shown in Table 11. No corrections have been made to ΔH_r of the sillimanite–kyanite reaction for Al/Si disorder in sillimanite. Although the discrepancies between the present volume data and those of Skinner *et al.* (1961) are relatively large, due to the uncertainties in enthalpy values, both volume sets are consistent with experimentally-determined thermodynamic properties of the aluminum silicates.

Table 9. Sillimanite, andalusite, and kyanite: molar volumes and $(\partial V/\partial T)_P$ slopes

	V (cm^3/mol)	$(\delta V/\delta T)_P$
Sillimanite	50.049(7)	7.230×10^{-4}
Andalusite	51.579(9)	12.926×10^{-4}
Kyanite	44.221(14)	11.774×10^{-4}

Table 11. Calculated and calorimetric reaction enthalpies at atmospheric pressure and equilibrium temperature for the aluminum silicate polymorphic inversion reactions

Reaction	T_{eq}	Slope (bars $deg.^{-1}$)	ΔH at T_{eq} (cals/mol.) Skinner et al.	Present Study	Calorimetric*
And.-Sill.	770°C	-13.97	800	670	670±230
Ky.-And.	220°C	12.49	1051	1043	956±200
Sill.-Ky.	326°C	20.19	-1647	-1617	-1720±170

*See text for sources.

Acknowledgments

We are indebted to Professor P. B. Moore, University of Chicago, and Mr. John S. White, Jr., Smithsonian Institution, for the sillimanite and kyanite samples respectively, and to Professors B. W. Evans and J. A. Vance, University of Washington, and Professor C. W. Burnham, Harvard University, for critical reviews. This research has been supported by NSF (Geochemistry) grant EAR 76-13373.

References

Anderson, P. A. M. and O. J. Kleppa (1969) The thermochemistry of the kyanite–sillimanite equilibrium. *Am. J. Sci., 267,* 285–290.

———, R. C. Newton and O. J. Kleppa (1977) The enthalpy change of the andalusite–sillimanite reaction and the Al_2SiO_5 diagram. *Am. J. Sci., 277,* 585–593.

Beger, R. M., C. W. Burnham and J. F. Hays (1970) Structural changes in sillimanite at high temperature (abstr.). *Geol. Soc. Am. Abstracts with Programs, 2,* 490–491.

Bond, W. L. (1951) Making small spheres. *Rev. Sci. Instrum., 22,* 344–345.

Brace, W. F., C. H. Scholz and P. N. LaMori (1969) Isothermal compressibility of kyanite, andalusite, and sillimanite from synthetic aggregates. *J. Geophys. Res., 74,* 2089–2098.

Burnham, C. W. (1963a) Refinement of the crystal structure of sillimanite. *Z. Kristallogr., 118,* 127–148.

——— (1963b) Refinement of the crystal structure of kyanite. *Z. Kristallogr., 118,* 337–360.

——— and M. J. Buerger (1961) Refinement of the crystal structure of andalusite. *Z. Kristallogr., 115,* 269–290.

Busing, W. R. and H. A. Levy (1964) The effect of thermal motion on the estimation of bond lengths from diffraction measurements. *Acta Crystallogr., 17,* 142–146.

Cromer, D. T. and J. B. Mann (1968) X-ray scattering factors

computed from numerical Hartree-Fock wave functions. *Acta Crystallogr., A24,* 321–324.

——— and D. Liberman (1970) Calculation of anomalous scattering factors for X-rays. *J. Chem. Phys., 53,* 1891–1898.

Finger, L. W. (1969) Determination of cation distribution by least-squares refinement of single-crystal X-ray data. *Carnegie Inst. Wash. Year Book, 67,* 216–217.

——— and E. Prince (1972) Neutron diffraction studies: andalusite sillimanite. *Carnegie Inst. Wash. Year Book, 71,* 496–500.

Greenwood, H. J. (1972) Al^{IV}–Si^{IV} disorder in sillimanite and its effects on phase relations of the aluminum silicate minerals. *Geol. Soc. Am. Mem., 132,* 553–571.

Hamilton, W. C. (1959) On the isotropic temperature factor equivalent to a given anisotropic temperature factor. *Acta Crystallogr., 12,* 609–610.

Hietanen, A. (1956) Kyanite, andalusite, and sillimanite in the schist in Boehls Butte quadrangle, Idaho. *Am. Mineral., 41,* 1–27.

Holdaway, M. J. (1971) Stability of andalusite and the aluminum silicate phase diagram. *Am. J. Sci., 271,* 91–131.

Kwak, T. A. P. (1971) The selective replacement of the aluminum silicates by white mica. *Contrib. Mineral. Petrol., 32,* 193–210.

McConnell, J. D. C. and D. McKie (1960) The kinetics of the ordering process in triclinic $NaAlSi_3O_8$. *Mineral. Mag., 32,* 436–454.

Naray-Szabo, St., W. H. Taylor and W. W. Jackson (1929) The structure of kyanite. *Z. Kristallogr., 71,* 117–130.

Navrotsky, A., R. C. Newton and O. J. Kleppa (1973) Sillimanite disordering enthalpy by calorimetry. *Geochim. Cosmochim. Acta, 37,* 2497–2508.

Ohashi, Y. and L. W. Finger (1973) Lattice deformations in feldspars. *Carnegie Inst. Wash. Year Book, 72,* 569–573.

Pankratz, L. B. and K. K. Kelley (1964) High temperature heat contents and entropies of andalusite, kyanite and sillimanite. *U.S. Bur. Mines Rept. Investigations 6370.*

Pauling, L. (1960) *The Nature of the Chemical Bond,* 3rd ed. Cornell University Press, New York.

Pitcher, W. S. (1965) The aluminum silicate polymorphs. In W. S. Pitcher and G. W. Flinn, Eds., *Controls of Metamorphism,* p. 327–341. Wiley, New York.

Quareni, S. and W. H. Taylor (1971) Anisotropy of the sodium atom in low albite. *Acta Crystallogr., 27B,* 281–285.

Skinner, B. J., S. P. Clark and D. E. Appleman (1961) Molar volumes and thermal expansions of andalusite, kyanite, and sillimanite. *Am. J. Sci., 259,* 651–668.

Taylor, W. H. (1928) The structure of sillimanite and mullite. *Z. Kristallogr., 68,* 503–521.

——— (1929) The structure of andalusite, Al_2SiO_5. *Z. Kristallogr., 71,* 205–218.

Weill, D. F. (1966) Stability relations in the Al_2O_3–SiO_2–Na_3AlF_6 system. *Geochim. Cosmochim. Acta, 30,* 223–227.

Winter, J. K., S. Ghose and F. P. Okamura (1977) A high-temperature study of the thermal expansion and the anisotropy of the sodium atom in low albite. *Am. Mineral., 62,* 921–931.

Woodland, B. G. (1963) Petrographic study of thermally metamorphosed pelitic rocks in the Burke area, north-eastern Vermont. *Am. J. Sci., 261,* 354–375.

Zen, E-an (1969) The stability relations of the polymorphs of aluminum silicate: a survey and some comments. *Am. J. Sci., 267,* 297–309.

Manuscript received, April 17, 1978;
accepted for publication, October 18, 1978.